J. Biochem. 120, 276-285 (1996)

In Vitro Refolding and Unfolding of Subunits of Electron-Transferring Flavoprotein: Characterization of the Folding Intermediates and the Effects of FAD and AMP on the Folding Reaction[1]

Kyosuke Sato, Yasuzo Nishina, and Kiyoshi Shiga

Department of Physiology, Kumamoto University School of Medicine, Honjo, Kumamoto, Kumamoto 860

Received for publication, February 9, 1996

Electron-transferring flavoprotein (ETF) from pig kidney is composed of two subunits (α and β, molecular weights of 33,000 and 29,000) and two small molecules, FAD and AMP. In this study, *in vitro* refolding and unfolding of the subunits of ETF were carried out with urea as the denaturing reagent. The refolding reaction of α and β was revealed to proceed kinetically in two steps: D⇄I→N, where D, I, and N denote the denatured, intermediate, and native forms, respectively. The features of the I forms of α and β, described below, are consistent with the concept of the so-called "molten globule state," which is frequently observed in protein refolding. (i) The conversion between D and I was very rapid. (ii) The I form showed as much secondary structure as the N form as judged from the far-UV circular dichroism. (iii) The solvent accessibility of the I form, estimated by the analysis of equilibrium unfolding experiments, was intermediate between those of the D and N forms. (iv) The standard free energy of the I form is almost the same as that of the D form. The refolding reaction progressed more slowly and the environment of the tryptophan chromophore was changed more drastically in β refolding than in α refolding. We previously reported that the reconstitution of holoETF from denatured subunits is speeded up by increasing the AMP concentration. In this study, the effects of AMP, FAD, and the other subunit on the single subunit folding were examined, but no effect was detected. This result suggests that AMP plays a role in a later process, namely, assembly of the four components (refolded α and β, FAD, and AMP).

Key words: AMP, electron-transferring flavoprotein, folding intermediate, subunit, urea denaturation.

Mammalian electron-transferring flavoprotein (ETF) is located in the mitochondrial matrix (*1*). ETF is a heterodimer (*2-5*) containing one flavin adenine dinucleotide (FAD) (*3-5*) and one AMP (*6-8*). These four components are bound tightly through non-covalent interactions. The molecular weight of each subunit was estimated by SDS-PAGE to be 31,100-33,500 for the α subunit and 25,100-30,000 for the β subunit (*2, 3, 5, 9*). The three-dimensional structure of ETF is still unknown and the location of the binding sites of FAD and AMP is also unclear at present.

The effect of AMP on the protein activity is unclear because the AMP-deficient ETF has the same activity as the holoETF (*6*). A role of AMP was suggested by an experiment on reconstitution of holoETF from denaturant-unfolded subunits: the binding of FAD to the apoprotein was made faster by raising the AMP concentration (*6*). The AMP presumably plays a role in folding or assembling ETF. In this study, we investigated the folding reactions of the subunits of ETF and the effect of AMP on these processes.

For many proteins, it has been found that *in vitro* refolding induced by a denaturant concentration jump proceeds in two steps, D⇄I→N: a folding intermediate (I) accumulates in an early period of the refolding from the denatured form (D) to the native form (N) (*10, 11*). This intermediate is the so-called "molten globule state" (*12*), which is characterized by native-like secondary structure but little formation of native tertiary structure. The I form is hardly detected in equilibrium unfolding experiments, but can be observed in kinetic folding experiments for many proteins. In this study, the I forms of α and β subunits were detected. We analyze the urea concentration-dependence of the D⇄I and I⇄N reactions, and discuss the structural and energetic features of the three states of the subunits.

MATERIALS AND METHODS

Materials—ETF was purified from pig kidney by the method of Gorelick *et al.* (*3*) with our modifications described previously (*13*). The α and β subunits of ETF were separated in urea-denatured forms by cation-exchange chromatography as described previously (*9*). The subunits were stored at 100 μM in 4 M urea solution containing 50 mM potassium phosphate, pH 7.6, 5% v/v glycerol, and 10 mM dithiothreitol (DTT). The DTT in the stock solution is indispensable for the restoration of the

[1] This work was supported in part by a Grant-in-Aid for Scientific Research from the Ministry of Education, Science, Sports and Culture of Japan.

Abbreviations: AMP, adenosine 5′-monophosphate; DTT, dithiothreitol; ETF, electron-transferring flavoprotein; FAD, flavin-adenine dinucleotide.

subunits to their native form (*6*). The subunits were stored at −18°C until used for experiments.

We verified that the subunits used in this study could revert to the holoprotein by means of the following experiment. Both the subunits in 4 M urea were diluted with buffer solution containing FAD and AMP to give the final conditions of 0.5 μM α and β, 2 μM FAD, 20 μM AMP, 0.04 M urea in 50 mM potassium phosphate buffer, pH 7.6, containing 5% v/v glycerol and 1 mM DTT. The restored holoETF quantified from the flavin fluorescence enhancement (*9*) always corresponded to more than 80% of the used subunits.

FAD obtained from Nacalai Tesque was further purified by C-18 reverse-phase HPLC as previously described (*6*). AMP and poly-L-lysine hydrochloride (mol. wt. 30,000-70,000) were purchased from Sigma. Glycyl-L-tyrosinamide acetate was from Wako Pure Chemical. Other chemicals were all from Nacalai Tesque.

General Methods—Concentrations were determined spectrophotometrically using the following molar extinction coefficients: $\varepsilon_{275} = 15{,}600\ M^{-1}\cdot cm^{-1}$ for α (*9*), $\varepsilon_{280} = 8{,}300\ M^{-1}\cdot cm^{-1}$ for β (*9*), $\varepsilon_{450} = 11{,}300\ M^{-1}\cdot cm^{-1}$ for FAD (*14*), and $\varepsilon_{260} = 15{,}400\ M^{-1}\cdot cm^{-1}$ for AMP (*15*).

Circular dichroism (CD) was measured with a JASCO J-600 spectropolarimeter equipped with a water-circulated cell holder. The instrument was calibrated with ammonium *d*-camphor-10-sulfonate as described in the instruction manual.

Fluorometric measurements were carried out with a Hitachi 850 fluorescence spectrophotometer equipped with a water-circulated cell holder. The fluorimeter was calibrated by using rhodamin-B and a light diffuser as described in the instruction manual.

Procedure for Refolding and Unfolding of Protein—All the buffer solutions used in this study were 50 mM potassium phosphate, pH 7.6, containing 5% v/v glycerol.

Protein refolding was initiated by rapid manual mixing of a measured volume of protein stock solution (5-20 μl) with the buffer solution (about 2 ml) containing 1 mM DTT and a suitable concentration of urea to give the intended final concentration. Protein unfolding was carried out by mixing the refolded protein and the buffer solution containing an appropriate concentration of urea to give the intended final concentration.

As reported previously (*9*), the refolded subunits without FAD and AMP are susceptible to aggregation at high concentration. We kept the concentration of the refolded subunits below 1 μM to avoid irreversible denaturation.

Refolding by the stopped-flow method was performed by using an RX. 1000 rapid kinetics spectrometer accessory (Applied Photophysics) and a Hitachi F-4500 fluorescence spectrophotometer. The protein stock solution and the buffer solution were mixed in 1:10 ratio.

Data Analysis—Obtained data were curve-fitted by non-linear least-squares analysis. The Gauss-Newton method was applied for the repeated approximation of the parameters in the non-linear fitting. The computer programs were originally written in language C, compiled by LSI C-86 compiler version 3.30c "tasting edition," and run on an NEC PC-9801 NS/T personal computer with an MS-DOS platform.

RESULTS

Unfolding-Refolding Equilibrium of ETF Subunits—Figure 1 shows the far-UV CD spectra of α and β in high and low concentrations of urea. The subunits show small CD signals in 6 M urea (trace **D**), suggesting the unordered conformation. In 0.02 M urea (trace **N**), the subunits acquire substantial CD signals, indicating the formation of ordered secondary structure.

The circles in Fig. 2 (upper) show the CD values of α (A) and β (B) at the equilibrium state in various urea concentrations. Figure 2 (lower) shows the values of protein fluorescence. Denaturation-renaturation transition is clearly observed between 1 and 2 M urea for both subunits, by both CD and fluorescence. The values indicated by open circles were obtained by dilution of the protein unfolded in 4 M urea to give the intended final urea concentration (refolding). The filled circles show the values obtained after addition of a high concentration of urea to the refolded subunit in 0.03 M urea to give the intended urea concentration (unfolding). The two plots obtained by unfolding and refolding coincide with each other, indicating that the *in vitro* refolding and unfolding of the subunits are essentially reversible.

Refolding Kinetics of ETF Subunits—Figure 3A shows the far-UV CD (upper) and protein fluorescence (lower) time courses of the refolding of α at 0.08 M urea and Fig. 3B shows those of β. The reaction curves were analyzed by least-squares analysis with a single exponential function:

$$Y(t) = (Y_0 - Y_\infty)e^{-k_{obs}t} + Y_\infty, \quad (1)$$

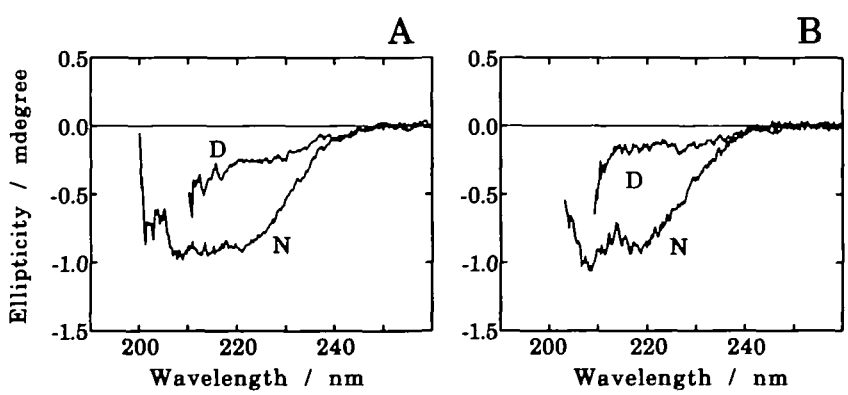

Fig. 1. **Far-UV circular dichroism spectra of α (A) and β (B).** Conditions were 0.5 μM α or β in 50 mM potassium phosphate buffer, pH 7.6, containing 5% v/v glycerol, 1 mM DTT, and 6 M (D) or 0.02 M (N) urea, at 25°C. The light path length was 1 mm.

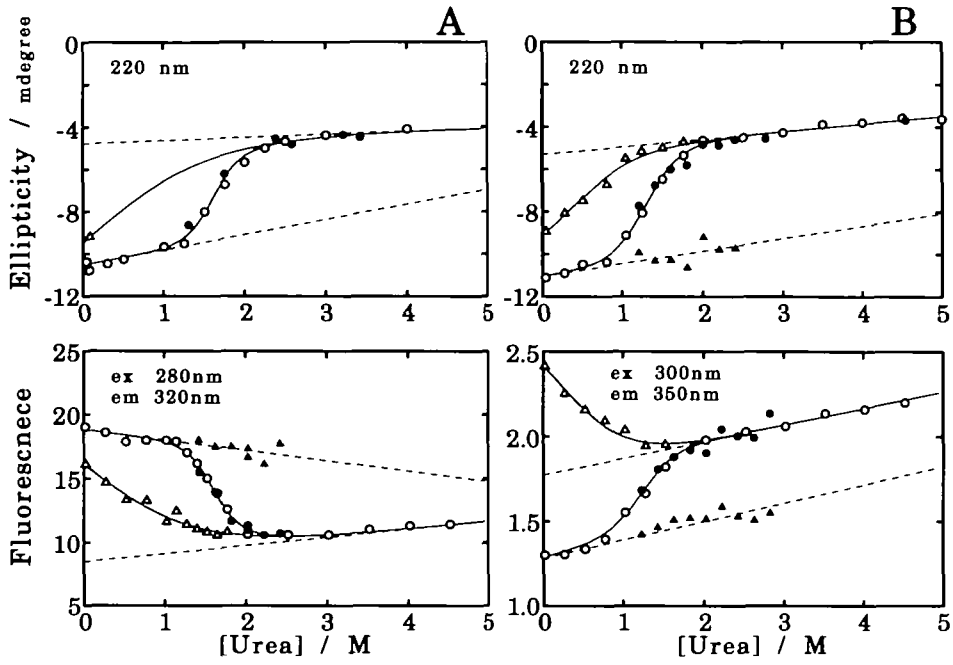

Fig. 2. **Equilibrium denaturation curves of α (A) and β (B).** Conditions were 0.5 μM subunit in 50 mM potassium phosphate buffer, pH 7.6, containing 5% v/v glycerol, 1 mM DTT, and the indicated concentration of urea, at 25°C. Refolding and unfolding reactions were detected by CD at 220 nm (upper) with a light path length of 1 cm and protein fluorescence (lower) measurements: the scale of the fluorescence represents the output value of the fluorimeter and the excitation and emission wavelengths are shown in the figure. Open marks show the values of refolding from 4 M urea; immediately after dilution (△) and at equilibrium (○). Filled marks show the values of unfolding from 0.03 M urea; immediately after the addition of urea (▲) and at equilibrium (●). The values shown by triangles (△ and ▲) were obtained as the thin arrows in Figs. 3 and 4.

where $Y(t)$, Y_0, and Y_∞ are the optical values at time t, at zero time, and at equilibrium, respectively, and k_{obs} is the observed rate constant of the reaction[2]. The thin curves in Fig. 3 are the best fit curves, showing good agreement with the recorded time courses. The k_{obs} values of the α refolding were calculated to be 0.13 s^{-1} for CD change and 0.12 s^{-1} for fluorescence change, and those of the β refolding were calculated to be 5.5×10^{-3} s^{-1} (CD) and 4.6×10^{-3} s^{-1} (fluorescence). The CD and fluorescence changes of each subunit thus showed good coincidence.

The protein should be in the unfolded form at zero time after dilution. The thick arrows in Fig. 3, A and B, indicate the optical values of the unfolded protein at 0.08 M urea (refolding condition). The CD and fluorescence values of the post-transition region (above 3 M urea) are dependent on urea concentration (Fig. 2). The values indicated by the thick arrows were obtained by linear extrapolation from the post-transition region to 0.08 M urea. [We measured the CD and fluorescence values of model compounds at several urea concentrations. As a model compound of denatured protein backbone, we chose poly-L-lysine at pH 4.8, which has an unordered conformation even in the absence of denaturants (*16*). As the models of the fluorophores of unfolded protein, *N*-acetyl-L-tryptophan ethyl ester and glycyl-L-tyrosinamide acetate were used. They all showed linear dependence on urea concentration at 0-6 M (data not shown). This result supports the above assumption that the CD and fluorescence of the unfolded forms change linearly with respect to urea concentration.] The thin arrows in Fig. 3, A and B, indicate the extrapolated values of the time courses to zero time (Y_0 values of Eq. 1). The two values indicated by thick and thin arrows disagree with each other for all four traces in Fig. 3, A and B. This observation indicates that the refolding reactions of the subunits do not follow a simple one-step refolding mechanism: a very rapid structural change occurs within the dead time (about 4 s) of the manual mixing. This rapid reaction was also undetectable by a fluorescence experiment using a stopped-flow apparatus with the dead time of less than 50 ms at 0.4 M urea.

The above observations can be explained by assuming a folding intermediate between the native and denatured forms. The equilibrium between the denatured form (D) and the intermediate form (I) is attained rapidly within the dead time of mixing, followed by a relatively slow change to attain the final equilibrium among the three forms, including the native folded form (N).

$$(D \underset{\text{rapid}}{\rightleftharpoons} I) \underset{\text{slow}}{\rightleftharpoons} N \qquad (2)$$

We use below the term "pre-equilibrium" to express the state where only D and I forms are in equilibrium and no molecule is present in N form. The open triangles in Fig. 2, A and B, show the Y_0 values, indicated by the thin arrows in Fig. 3, at various urea concentrations. According to the model of Scheme 2, the Y_0 values are the optical values at

TABLE I. **Parameters for the equilibrium unfolding of the ETF subunits.** The equilibrium denaturation data for α and β in 50 mM potassium phosphate, pH 7.6, 5% v/v glycerol, 1 mM DTT, and various concentrations of urea at 25°C were analyzed according to the reaction model, D⇌I⇌N. The standard free energy change ($\Delta G'$) of transition is given by $\Delta G' = \Delta G'^{\circ} - \Delta A[\text{urea}] = -\Delta A([\text{urea}] - C_m)$. ΔA is a measure of the dependence of $\Delta G'$ on urea concentration, C_m is the urea concentration at the transition midpoint, and $\Delta G'^{\circ}$ is the standard free energy change in the absence of urea.

	ΔA/kJ·mol^{-1}·M^{-1}	C_m/M	$\Delta G'^{\circ}$/kJ·mol^{-1}
α D→I	−3.5±1.2	0.06±0.74	−0.2±2.6
I→N	−11.9±0.1	2.06±0.01	−24.5±0.3
D→N	−15.4±1.3	1.60±0.31	−24.7±2.9
β D→I	−5.7±1.5	0.18±0.31	−1.0±1.4
I→N	−4.5±0.0	2.66±0.01	−11.9±0.2
D→N	−10.2±1.5	1.26±0.34	−12.9±1.6

[2] In this paper, the subscripts "∞" and "0" of Y represent infinite time and zero time, respectively. On the other hand, the superscript "0" of Y, $\Delta G'$, and k indicates that the urea concentration is 0 M. The superscript "°" represents the standard state, so that G' denotes the standard free energy.

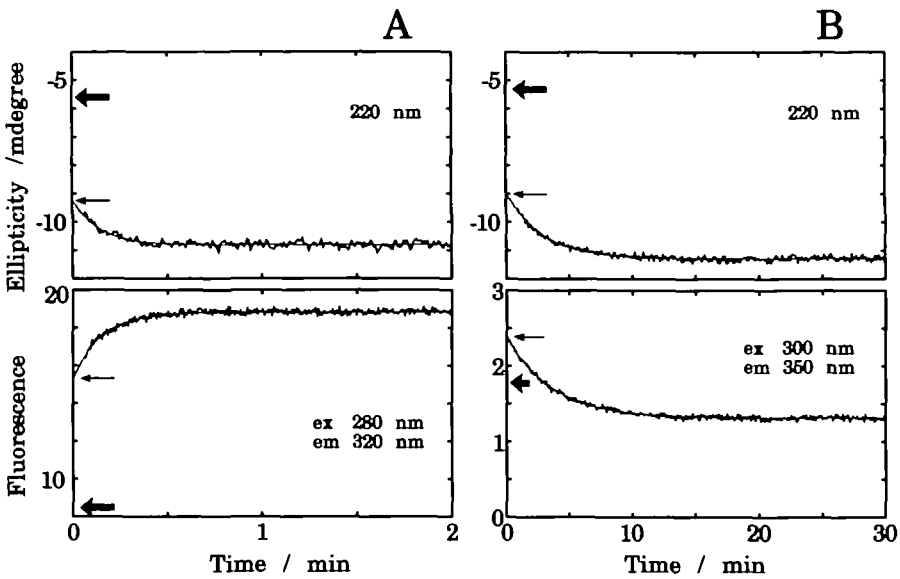

Fig. 3. **Refolding time courses of α (A) and β (B).** A solution of 100 μM α or β in 4 M urea was added to the buffer solution in the spectrophotometric cell at zero time. The final conditions were 0.5 μM α or β in 50 mM potassium phosphate buffer, pH 7.6, containing 5% v/v glycerol, 1 mM DTT, and 0.08 M urea, at 25°C. Reactions were followed by CD at 220 nm (upper) with a light path length of 1 cm and protein fluorescence (lower) at the excitation and emission wavelengths shown in the figure. The CD time course of α refolding was obtained by accumulation of eight runs. Others were obtained by single runs. The thin curves are the best fit curve obtained by least-squares analysis with a single exponential function, $Y(t) = (Y_0 - Y_\infty)\exp(-k_{obs}t) + Y_\infty$, where Y_0, Y_∞, and k_{obs} are the parameters to be obtained. The thin arrows show the Y_0 values. The thick arrows show the expected values of the denatured form at 0.08 M urea; these values were obtained by linear extrapolation from the post-transition region (above 3 M urea) of the equilibrium denaturation curve (Fig. 2).

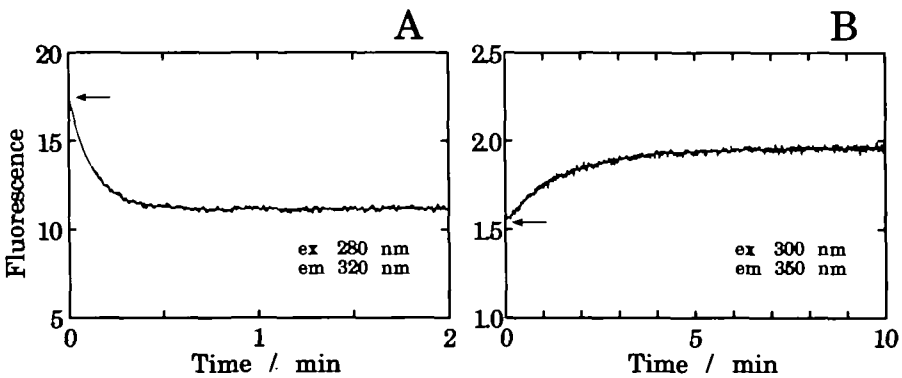

Fig. 4. **Unfolding time courses of α (A) and β (B) detected by protein fluorescence measurement.** First, α and β were allowed to refold at 0.03 M urea. At zero time, 1.4 ml of 0.71 μM refolded subunit was mixed with 0.6 ml of 6.67 M urea. The final conditions were 0.5 μM subunit, 2.02 M urea, 50 mM potassium phosphate, pH 7.6, 5% v/v glycerol, and 1 mM DTT, at 25°C. The excitation and emission wavelengths are shown in the figure. The thin curves are the best fit curves obtained by least-squares analysis with a single exponential function, $Y(t) = (Y_0 - Y_\infty)\exp(-k_{obs}t) + Y_\infty$. The arrows show the Y_0 values.

pre-equilibrium between D and I, so that the open triangles in Fig. 2, A and B represent the D⇄I transition curve. At low urea concentration, the Y_0 value is very different from the optical values of the unfolded form (the broken line extended from the post-transition region). This indicates that the equilibrium of D⇄I was shifted rightward at lower urea concentration.

Unfolding Kinetics of ETF Subunits—According to the model of Scheme 2, the unfolding reaction from N form should be monophasic: the rapid change within the dead time of mixing must not be observed, unlike the case of refolding. Figure 4 shows the unfolding time course of α (A) and β (B) caused by the urea concentration jump from 0.03 to 2.02 M. The recorded time courses were fitted well by a single exponential function (Eq. 1); the thin curves in Fig. 4 show the best fit curves. The arrows in Fig. 4 show the extrapolated values of the time courses to zero time (Y_0 values of Eq. 1). The Y_0 values of unfolding at several urea concentrations are shown by the filled triangles in Fig. 2. The open circles in the pre-transition region and the filled triangles lie along the same line. This indicates that the optical values of the refolded form are linearly dependent on urea concentration and that rapid changes within the dead time of unfolding do not occur. This result supports the validity of the reaction model of Scheme 2.

Figure 5 shows the k_{obs} values of refolding (open marks) and unfolding (filled marks) of α and β detected by CD (triangles) and fluorescence (circles). The values obtained by CD and fluorescence are in good agreement with each other, implying that both techniques detected the same reaction. These data are numerically analyzed later.

Data Analyses of the Refolding-Unfolding Equilibrium Curves—The data of equilibrium unfolding curves (Fig. 2) of α (A) and β (B) were analyzed according to the following reaction model:

$$D \overset{K_{DI}}{\rightleftharpoons} I \overset{K_{IN}}{\rightleftharpoons} N,$$

where K_{DI} and K_{IN} are the equilibrium constants of the respective reaction.[3] Equilibrium constants are related with standard free energy changes of D→I and I→N transitions, ΔG°_{DI} and ΔG°_{IN}, by the equations,

$$K_{DI} = \exp\left(-\frac{G^\circ_{DI}}{RT}\right) \quad (3)$$

[3] In this paper, the subscript "XY" indicates that the value refers to the reaction, X→Y. This also applies to ΔG°_{XY}, $C_{m,XY}$, and ΔA_{XY}.

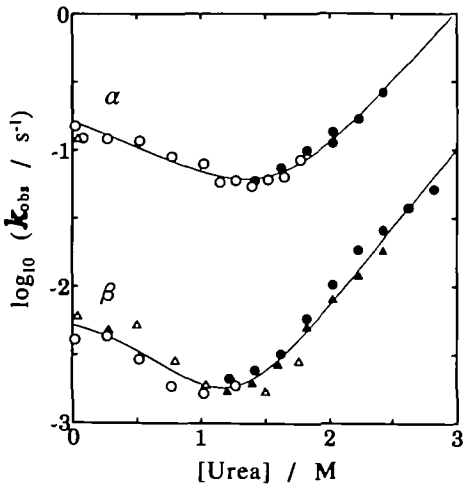

Fig. 5. **Observed rate constants for refolding and unfolding of α and β at various urea concentrations.** Refolding and unfolding time courses, such as Figs. 3 and 4, were analyzed by curve fitting with a single exponential function, $Y(t)=(Y_0-Y_\infty)\exp(-k_{obs}t)+Y_\infty$. The obtained k_{obs} values (observed rate constant) at various urea concentrations were plotted in this figure. Different symbols indicate the different methods: refolding from 4 M urea detected by protein fluorescence (○), refolding detected by CD (△), unfolding from 0.03 M urea detected by protein fluorescence (●), and unfolding detected by CD (▲). Conditions were 0.5 μM subunit in 50 mM potassium phosphate buffer, pH 7.6, containing 5% v/v glycerol, 1 mM DTT, and the indicated concentration of urea, at 25°C. The k_{obs} values depending on the urea concentration were analyzed as described in the text, and the results of the best fit are shown by the curves, which were drawn according to Eqs. 11 with Eqs. 12 and 13 and the values listed in Table II.

$$K_{IN}=\exp\left(-\frac{G^*_{IN}}{RT}\right) \quad (4)$$

where R is the gas constant and T is absolute temperature (273.16+25.0 K, in the present case). According to the most frequently employed method, the standard free energy change of transition was assumed to be linearly dependent on urea concentration (*17, 18*).

$$\Delta G^*_{DI}=-\Delta A_{DI}([\text{urea}]-C_{m,DI}) \quad (5)$$

$$\Delta G^*_{IN}=-\Delta A_{IN}([\text{urea}]-C_{m,IN}) \quad (6)$$

where ΔA indicates the dependence of ΔG^* on urea concentration and C_m is the urea concentration at the transition midpoint, where the concentrations of the two states are the same. Brackets represent molar concentration of the substance enclosed by them. The plots at the pre- and post-transition regions shown in Fig. 2 have slopes, probably due to a solvent effect. We assumed that the optical signals of pure D, I, and N forms are linearly dependent on urea concentration.

$$Y_X=Y^0_X+m_X[\text{urea}] \quad (X=D, I, \text{or } N)$$

The optical values at equilibrium (Y_{eq}) are represented by

$$Y_{eq}=\frac{Y_D+K_{DI}Y_I+K_{DI}K_{IN}Y_N}{1+K_{DI}+K_{DI}K_{IN}} \quad (7)$$

because the ratio of the concentrations of the three forms at equilibrium is related to the equilibrium constants as follows: $[D]:[I]:[N]=1:K_{DI}:K_{DI}K_{IN}$. The optical values at pre-equilibrium between D and I forms are given by

TABLE II. **Parameters for the kinetic constants of refolding and unfolding of the ETF subunits.** The observed rate constants (k_{obs}) of refolding and unfolding of α and β in 50 mM potassium phosphate, pH 7.6, 5% v/v glycerol, 1 mM DTT, and various concentrations of urea at 25°C were analyzed according to the model: $D \underset{k_-}{\overset{K_{DI}}{\rightleftharpoons}} I \underset{k_-}{\overset{k_+}{\rightleftharpoons}} N$. The kinetic constants in this model are related to the parameters in the table by the equations, $k_+=k^0_+\exp(\Delta A_{IT}\cdot[\text{urea}]/RT)$ and $k_-=k^0_-\exp(\Delta A_{NT}\cdot[\text{urea}]/RT)$.

k^0_+/s^{-1}	$\Delta A_{IT}/kJ\cdot mol^{-1}\cdot M^{-1}$	k^0_-/s^{-1}	$\Delta A_{NT}/kJ\cdot mol^{-1}\cdot M^{-1}$
α $(3.0\pm0.1)\times10^{-1}$	-0.15 ± 0.33	$(9.7\pm4.8)\times10^{-4}$	5.74 ± 0.57
β $(8.8\pm0.8)\times10^{-3}$	0.58 ± 0.50	$(3.4\pm1.2)\times10^{-5}$	6.64 ± 0.41

$$Y_{0,refold}=\frac{Y_D+K_{DI}Y_I}{1+K_{DI}}, \quad (8)$$

because the protein exists in an equilibrium of D and I forms ($[D]:[I]=1:K_{DI}$) and no molecules exist in the N form at pre-equilibrium. The extrapolated values of the unfolding time courses to zero time are represented by

$$Y_{0,unfold}=Y_N, \quad (9)$$

because all the molecules are in the N form at zero time of unfolding. The data shown by the filled and open circles in Fig. 2 were fitted by using Eq. 7, the open triangles by Eq. 8, and the filled triangles by Eq. 9. All the CD and fluorescence data for each subunit were simultaneously curve-fitted to obtain the four thermodynamic parameters (ΔA_{DI}, $C_{m,DI}$, ΔA_{IN}, $C_{m,IN}$) with the other ten parameters (Y^0_D, m_D, Y^0_N, m_N, and Y^0_I for both CD and fluorescence). [When m_I for CD and fluorescence were included in the parameters to be obtained, the parameters diverged during the repetitive approximation. Thus, these two values were kept equal to zero during the calculation. This operation does not cause serious errors in the other parameters: even when the m_I values were set at $\pm2m_N$ or $\pm2m_D$, the other parameters were not changed significantly. The small importance of the m_I values can be ascribed to the fact that the D→I transition is only about half completed even at zero urea concentration.] The curves and lines in Fig. 2 show the results of the least-squares analysis; they fit well with the experimental data. Table I shows the obtained thermodynamic parameters. The standard free energy change at 0 M urea was calculated by use of the equation, $\Delta G^{*0}=\Delta A\times C_m$. The parameters for D→N transition were calculated from those for D→I and I→N transitions, that is, $\Delta G^{*0}_{DN}=\Delta G^{*0}_{DI}+\Delta G^{*0}_{IN}$, $\Delta A_{DN}=\Delta A_{DI}+\Delta A_{IN}$, and $C_{m,DN}=\Delta G^{*0}_{DN}/\Delta A_{DN}$.

The CD values of the pure D, I, and N forms were estimated as $Y^0_D=-4.8\pm0.5$ millidegrees (m°), $Y^0_I=-13.8\pm5.1$ m°, and $Y^0_N=-10.5\pm0.2$ m° for α and $Y^0_D=-5.2\pm0.3$ m°, $Y^0_I=-10.6\pm1.4$ m°, and $Y^0_N=-11.2\pm0.2$ m° for β. The Y^0_I values are near to the Y_N values rather than the Y_D values. This result indicates that the I form of each subunit has secondary structure as substantial as that of the N form.

Data Analyses of Refolding-Unfolding Kinetic Rate— From the kinetic experiments described above, Scheme 10 is proposed as the reaction model of the refolding-unfolding of α and β.

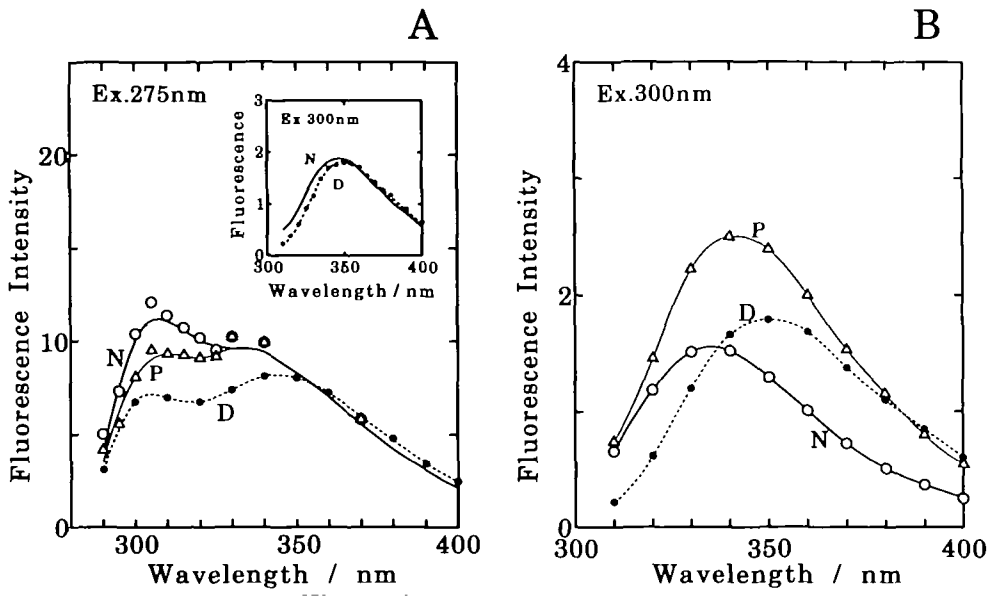

Fig. 6. **Fluorescence spectra of α (A) and β (B) at the different stages of refolding at 0.02 M urea.** All the spectra are those under the conditions of 0.5 μM subunit in 50 mM potassium phosphate buffer, pH 7.6, containing 5% v/v glycerol, 1 mM DTT, and 0.02 M urea, at 25°C. The excitation wavelengths are shown in the figure. The scale of the ordinate represents the output value of the fluorimeter. Spectra of the denatured form were recorded at several urea concentrations above 3 M. The plots of fluorescence values at each detection wavelength *vs.* urea concentration were linearly extrapolated to 0.02 M urea, and the extrapolated values are shown by the symbol ●. The expected spectrum of the denatured form (curve **D**) at 0.02 M urea was obtained by joining these filled circles. The time course of the subunit refolding initiated by dilution of the urea (4→0.02 M) was recorded at various detection wavelengths. These time courses were curve-fitted with the function, $Y(t)=(Y_0-Y_\infty)\exp(-k_{obs}t)+Y_\infty$. The obtained Y_0 values (fluorescence values extrapolated to zero time from the time courses) are shown by the symbol △ and the Y_∞ values (fluorescence values at infinite time) by the symbol ○. The spectrum at pre-equilibrium between D and I forms (curve **P**) was drawn by joining the open triangles. The spectrum of native form (curve **N**) was measured by wavelength scanning after the refolding equilibrium was attained.

$$\mathrm{D} \underset{\text{rapid}}{\overset{K_{DI}}{\rightleftharpoons}} \mathrm{I} \underset{k_-}{\overset{k_+}{\rightleftharpoons}} \underset{\text{slow}}{\mathrm{N}} \qquad (10)$$

The reaction D⇄I is much more rapid than the reaction I⇄N. Thus, the reaction D⇄I should be in equilibrium at any time during the recorded time course. The observed rate constant of the refolding and unfolding is related with the K_{DI}, k_+, and k_- values by the equation,

$$k_{obs}=\frac{K_{DI}}{1+K_{DI}}k_+ + k_- . \qquad (11)$$

[Assuming that the sum of the concentrations of D, I, and N is c, $[D]+[I]=c-[N]$. Because $[D]:[I]=1:K_{DI}$ at any time, the concentration of I is related with that of N by the equation, $[I]=K_{DI}(c-[N])/(1+K_{DI})$. Equation 11 is obtained by solving the differential equation, $d[N]/dt=k_+[I]-k_-[N]$, *i.e.*, $d[N]/dt=-\{K_{DI}k_+/(1+K_{DI})+k_-\}[N]+cK_{DI}k_+/(1+K_{DI})$.] According to the frequently employed method (*18*), we used transition state theory to characterize the dependence of the rate constants on urea concentration. The reactions I→N and N→I can be represented microscopically as

$$\mathrm{I} \underset{\text{equilibrium}}{\rightleftharpoons} \mathrm{T}^* \longrightarrow \mathrm{N}$$

$$\mathrm{N} \underset{\text{equilibrium}}{\rightleftharpoons} \mathrm{T}^* \longrightarrow \mathrm{I}$$

where T* is the transition state between the I and N forms. The kinetic constant is related with the standard free energy difference between the transition state and the reactant, $\Delta G^\circ_{IT^*}$ and $\Delta G^\circ_{NT^*}$, by the equations,

$$k_+=\frac{k_B T}{h}\exp\left(-\frac{G^\circ_{IT^*}}{RT}\right)$$

$$k_-=\frac{k_B T}{h}\exp\left(-\frac{G^\circ_{NT^*}}{RT}\right)$$

where k_B and h are the Boltzman and Planck constants. As described above for the equilibrium of D⇄I and I⇄N, the standard free energy change of activation is also assumed to be linearly dependent on urea concentration.

$$\Delta G^\circ_{IT^*}=\Delta G^{\circ 0}_{IT^*}-\Delta A_{IT^*}[\text{urea}]$$

$$\Delta G^\circ_{NT^*}=\Delta G^{\circ 0}_{NT^*}-\Delta A_{NT^*}[\text{urea}]$$

Thus, the rate constants are related with urea concentration as shown by Eqs. 12 and 13.

$$k_+=k_+^0\exp\left(\frac{\Delta A_{IT^*}}{RT}[\text{urea}]\right) \qquad (12)$$

$$k_-=k_-^0\exp\left(\frac{\Delta A_{NT^*}}{RT}[\text{urea}]\right), \qquad (13)$$

where k_+^0 and k_-^0 are the rate constants at zero urea concentration and ΔA_{IT^*} and ΔA_{NT^*} are the urea concentration dependencies of the standard free energy change of activation of the I and N forms. The log k_{obs} data in Fig. 5 were fitted with Eq. 11 (together with Eqs. 12 and 13, and the K_{DI} values calculated by use of Eqs. 3 and 5 with the parameters listed in Table I). The curves in Fig. 5 show the result of the fitting, well explaining the experimental results. The obtained k_+^0, ΔA_{IT^*}, k_-^0, and ΔA_{NT^*} values are shown in Table II.

Fluorescence Spectral Changes of Tryptophan and Tyrosine Chromophores of the α and β Subunits during Refolding—As a probe for the structures of the three states (N, I, and D forms) of each subunit, the protein fluorescence spectra were measured at different stages of refolding. We previously (*9*) estimated the aromatic amino acid contents of each subunit of pig kidney ETF as one tryptophan and six tyrosines in α and one tryptophan and one tyrosine in β by analyses of the UV absorption spectra of the guanidine-denatured subunits. The fluorescence of tryptophan and

TABLE III. **Degree of polarization of tryptophan fluorescence of the ETF subunits in different states.** The excitation and detection wavelengths were 300 and 350 nm, respectively. The degree of polarization (p) was obtained as $p=(I_{\parallel}-I_{\perp})/(I_{\parallel}+I_{\perp})$, where $I_{\parallel}$ and $I_{\perp}$ are polarized emission intensity parallel and perpendicular, respectively, to a vertically polarized excitation beam. The dependency of the photomultiplier sensitivity on the angle of emission polarization was corrected for by using the output values of vertically and horizontally polarized emission with horizontally polarized excitation. [a]The D form in 4 M urea. [b]At pre-equilibrium between D and I forms immediately after dilution at 0.02 M urea. [c]The N form in 0.02 M urea. [d]No significant changes of $I_{\parallel}$ and $I_{\perp}$ were detected during the time course of α refolding, so the value of p at pre-equilibrium was judged to be similar to that of N form.

	D[a]	Pre-equilibrium[b]	N[c]
α	0.064	0.13[d]	0.134
β	0.075	0.188	0.232

tyrosine can be distinguished by changing the excitation wavelength: only the tryptophan chromophore is excited at 300 nm, while both tyrosine and tryptophan are excited at lower wavelength.

The inset of Fig. 6A shows the tryptophan fluorescence spectra of α. Curve **N** is the spectrum of the N form measured at 0.02 M urea, where almost all molecules are in N state (see Fig. 2). Curve **D** is the expected spectrum of the D form at 0.02 M urea. [The fluorescence spectrum of the D form can be measured only in the post-transition region. We recorded the spectra at several points above 3 M urea. The fluorescence values at each wavelength *vs.* urea concentration were linearly fitted, and the extrapolated value to 0.02 M urea is shown in the figure by closed circles. Curve **D** was drawn on this basis.] Curve **D** shows a peak at 350 nm, like free tryptophan (*19*), suggesting that the tryptophan chromophore of the D state is exposed to the solvent and thus supporting the view that the D form is almost completely unfolded. The tryptophan fluorescence of the N form shows a peak at 344 nm with a similar peak intensity to the D form: the tryptophan fluorescence does not greatly differ between the N and D forms. The slight blue shift of the spectrum of the N form suggests a hydrophobic environment of the tryptophan chromophore buried in the N form (*20*). For the purpose of obtaining the spectrum at the pre-equilibrium state between the D and I forms, the fluorescence time course of the α refolding was monitored at several detection wavelengths from 310 to 400 nm with 300-nm excitation, each for 2 min. However, no significant fluorescence change was detected at any of the detection wavelengths, indicating that the tryptophan spectrum at immediately after the dilution was almost the same as that of the N form. The tryptophan fluorescence of α is changed only slightly during the whole refolding process.

Figure 6A shows the spectra of α excited at 275 nm. Curve **D** shows the spectrum of the D form at 0.02 M urea. It contains a large contribution of the tyrosine fluorescence, which shows a peak at around 305 nm, besides the tryptophan fluorescence. The solid curve **N** shows the spectrum of the N form recorded at 0.02 M urea. It has a peak at about 307 nm. The spectral difference between N and D is mainly due to the substantial intensification of the tyrosine fluorescence accompanying the D→N transition. The spectrum at pre-equilibrium between the D and I forms at 0.02 M urea was obtained from the time course of refolding detected at various wavelengths. The Y_0 and Y_∞ values calculated by curve fitting with Eq. 1 are shown in Fig. 6A by triangles and circles, respectively. The circles agree well with curve **N** measured by wavelength scanning, as expected. The spectrum at pre-equilibrium (curve **P**) is intermediate between the spectra of the N and D forms. The tyrosine fluorescence is more sensitive than the tryptophan fluorescence to the conformational change of α.

Figure 6B shows the tryptophan fluorescence change during the β refolding. The spectrum of the D form (curve **D**) shows a peak at 350 nm as in the case of α. At the pre-equilibrium between the D and I forms (curve **P**), the tryptophan fluorescence intensity was greatly enhanced and blue-shifted compared with the D form, suggesting a hydrophobic environment of tryptophan in the I form. The N form (**N**) shows a blue-shifted (peak at 335 nm) and slightly quenched tryptophan fluorescence as compared with the D form. Tryptophan fluorescence of β was substantially quenched by I→N transition. The tyrosine fluorescence change upon the transitions of β could not be detected because of the low intensity of tyrosine fluorescence due to its low content in β. Tryptophan fluorescence is a good probe to follow the refolding reaction of β.

The degrees of polarization of tryptophan fluorescence of α and β were also measured and the results are summarized in Table III. The polarization for the D form in 4 M urea was very small and similar between α and β, reflecting the rapid movement of the fluorophore in the D forms of both subunits. The polarization of the N form in 0.02 M urea is higher than that of the D form, reflecting the restriction of movement by the protein folding. The value of the N form of α (0.134) is significantly lower than that in the case of β (0.232). This result is consistent with the spectral features of the subunits: the tryptophan fluorescence spectrum of α was changed only slightly by the refolding (blue-shifted by only 6 nm, inset of Fig. 6A), while that of β was changed greatly (blue-shifted by 15 nm, Fig. 6B). The value of degree of polarization at pre-equilibrium between the D and I forms of α was almost the same as for the N form, while that of β was intermediate between those of the D and N forms.

Effects of AMP, FAD, and the Other Subunit on Subunit Folding—ETF contains two non-protein components, FAD and AMP (*6*). To examine whether FAD and AMP affect the folding reaction of each subunit, the denatured subunits were refolded in the presence of FAD and/or AMP to give final concentrations of 0.5 μM for subunits and 0.08 M for urea. The refolding of α was monitored in terms of tyrosine fluorescence change (280-nm excitation and 305-nm detection) and that of β was monitored in terms of tryptophan fluorescence change (300-nm excitation and 350-nm detection). The recorded time courses were fitted by a single exponential function (Eq. 1) and the parameters Y_0, Y_∞, and k_{obs} were obtained. The tested concentrations of FAD and AMP, respectively, were (i) 0 and 0 μM, (ii) 0 and 2 μM, (iii) 0 and 20 μM, (iv) 2 and 0 μM, (v) 20 and 0 μM, (vi) 2 and 2 μM, and (vii) 20 and 20 μM. In all cases, the subunit refolding was not affected by the ligands with respect to the parameters (Y_0, Y_∞, and k_{obs}) of the time course. [The observed Y_0 and Y_∞ values were corrected for the inner filter effect as described previously (*9*).]

The effect of the subunit on the refolding of the other subunit was also examined. To test the effect of β on α

refolding, two types of experiments were carried out: (i) β was diluted together with α and (ii) β was diluted at 20 min before the α dilution. The final concentrations were fixed at 0.5 μM for the subunits and 0.08 M for urea throughout these experiments. When the effect of α on β refolding was tested, the order of dilution was the reverse. [The refoldings of α and β were monitored by using different excitation and detection wavelengths as described above. In addition, the refolding rates of both subunits are very different (α refolds faster than β by a factor of 24; see Fig. 3). Therefore the refoldings of α and β can be monitored separately, even when both subunits are refolded simultaneously.] In all cases, the subunit refolding was not affected by the presence of the other subunit.

DISCUSSION

Energetic and Structural Changes of the Subunits during the Refolding—The urea-induced unfolding shown in Fig. 2 was analyzed by assuming that the standard free energy changes of the D→I and I→N transitions are linearly dependent on urea concentration, as represented by Eqs. 5 and 6. Those equations can be transformed to

$$\Delta G^{*}_{XY} = \Delta G^{*0}_{XY} - \Delta A_{XY}[\text{urea}], \quad (XY = DI, IN, \text{or } DN)$$

where ΔG^{*0} is the standard free energy change at 0 M urea. The symbol Δ with G°_{XY} and G^{*0}_{XY} represents the change accompanying the reaction X→Y, namely, $\Delta G^{\circ}_{XY} = G^{\circ}_{Y} - G^{\circ}_{X}$ and $\Delta G^{*0}_{XY} = G^{*0}_{Y} - G^{*0}_{X}$. A similar situation applies to ΔA_{XY} (Eq. 14), assuming that the standard free energy of each form also linearly depends on urea concentration (Eq. 15).

$$\Delta A_{XY} = A_Y - A_X \quad (14)$$

$$G^{\circ}_{X} = G^{*0}_{X} - A_X[\text{urea}] \quad (X = D, I, \text{or } N) \quad (15)$$

The interaction between protein and urea molecule can be considered in terms of binding (*21, 22*). The linear dependence of G°_{X} on urea concentration represented by Eq. 15 can be explained by assuming that many binding sites with very low affinity for urea are distributed on the protein surface. Therefore the value of A_X in Eq. 15 can be interpreted as the global affinity of the solvent-accessible surface of the X form for urea. For example, in the case of the D→N transition of general proteins, it is known that the ΔG°_{DN} value increases upon raising the urea concentration. This destabilization of the N form arises from the lower urea affinity of the N form than the D form ($A_N < A_D$, *i.e.*, $\Delta A_{DN} < 0$). The decrease of A on D→N transition can be explained by the burying of the protein surface of the D form into the interior of the N form. In other words, the A value reflects the solvent-accessible surface area of the protein. A decrease of the A value is indicative of the organization of structured conformation.

Figure 7 shows the changes of A (A) and G^{*0} (B) values of α and β along their folding pathways. The values are represented by the difference with respect to the D form. Figure 7B shows that the I form of each subunit is almost equal in free energy to the D form. Figure 7A shows that the global surface affinity for urea (or the solvent-accessible surface area) of the I form is intermediate between those of the D and N forms. In addition, it has been suggested that the I form is almost equivalent to the N form in secondary structure content (see the last part of the fourth section of

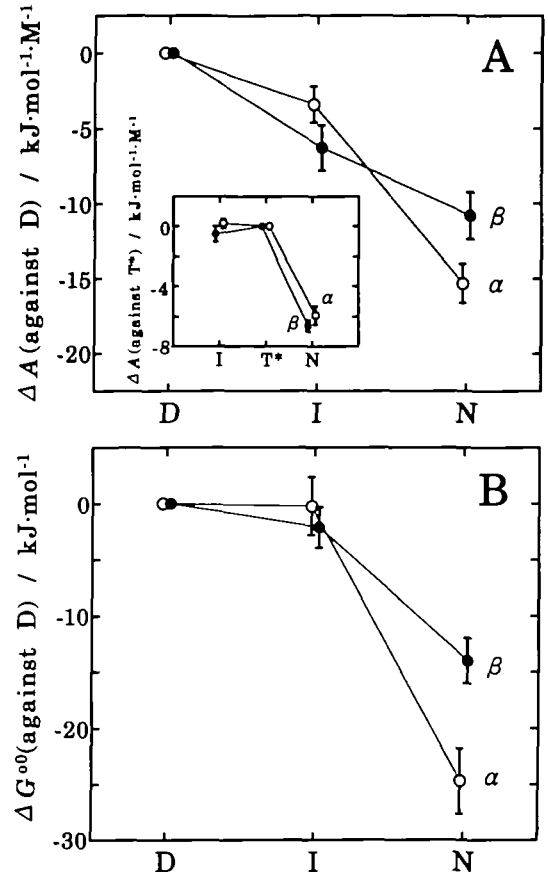

Fig. 7. **Reaction profile of A (A) and G^{*0} (B) of the subunits.** The values of (ΔA_{DI} and ΔG^{*0}_{DI}) and (ΔA_{DN} and ΔG^{*0}_{DN}) listed in Table I are plotted as the values for the I and N forms, respectively. G^{*0} is the standard free energy in the absence of urea. A is the measure of the dependence of G^{*} on urea concentration, and thus can be related to the solvent-accessible surface area of the individual forms of the subunits (see "DISCUSSION"). Inset: The values of $-\Delta A_{IT^*}$ and $-\Delta A_{NT^*}$ listed in Table II are plotted as the values for the I and N forms, respectively.

"RESULTS"). As a result, by the D→I transition, the subunits acquire almost the complete secondary structure with little consumption of free energy and with some burying of residues. Most of the free energy difference between the D and N forms is used to generate the tertiary structure during the I→N change. These characters of the I form of both subunits are consistent with the concept of the so-called "molten globule state," which is characterized by native-like secondary structure and little tertiary structure, like the denatured form (*10-12*).

The inset of Fig. 7A shows the change of A value during the reaction from I to N by way of the transition state (I→T*→N). The A values are represented by the difference with respect to the T* form. For the β subunit, the difference of A value between the I and N forms ($\Delta A_{IN} = -6.1$ kJ·mol^{-1}·M^{-1}) obtained from the kinetic data is in good agreement with the value ($\Delta A_{IN} = -4.5$ kJ·mol^{-1}·M^{-1}) obtained from the equilibrium data. This agreement supports the validity of the kinetic model (scheme 10) for β. The inset of Fig. 7A shows that structure of T* of β is similar to the I form rather than the N form with respect to the solvent-accessible surface area. The T* form of β may

have a distorted conformation which resembles the I form. On the other hand, for α, the value ($\Delta A_{IN} = -5.9$ kJ·mol^{-1}·M^{-1}) obtained from the kinetic data is significantly different from the value ($\Delta A_{IN} = -11.9$ kJ·mol^{-1}·M^{-1}) obtained from the equilibrium data. This disagreement may reflect a deficiency in scheme 10 for α. It is possible that another intermediate exists between the N and D forms.

The structure of the subunits can be evaluated to some extent from the protein fluorescence change during the refolding. The spectral change of the single tryptophan during the refolding is strikingly different between α and β (Fig. 6): the α tryptophan is only slightly reflective of the conformational change, whereas the β tryptophan is very sensitive. This suggests that the environment of the β tryptophan changes considerably with both D→I and I→N transitions, while that of the α tryptophan does not change so much. The result on the degree of polarization of tryptophan fluorescence (Table III) supports this idea. The lower value of the N form for α than for β suggests that the tryptophan side chain of α is located at an outer region and can move more rapidly, while that of β is more deeply buried and its movement is restricted.

Effects of FAD and AMP on Subunit Folding—We are interested in the function of AMP in ETF. It had been believed for many years that the only non-protein component of ETF is FAD, until the recent discovery that ETF also contains AMP (*6, 7*). ETF is a mitochondrial enzyme which serves as a part of the energy-producing system, so it seems physiologically significant that AMP is contained in ETF. However, the physiological role of AMP is still uncertain, because AMP-deficient ETF shows the same catalytic activity as the holoprotein of ETF in the standard assay system (*6*). One clue to the AMP function is the observation that the rate of formation of the holoprotein is accelerated by raising the AMP concentration during the *in vitro* reconstitution (*6*). Therefore, it is of interest to locate the target of AMP in the reconstitution pathway. In those experiments, the subunits unfolded by denaturants were diluted with buffer solution containing FAD and AMP, and thus the refolding occurred in the presence of FAD and AMP. For clarity, we should consider the reconstitution reaction as two distinct processes, (i) refolding of α and β and (ii) assembly of the four components (refolded subunits, FAD, and AMP). The present study was focused on the former process.

In this paper, we showed that AMP has no effects on the refolding reaction of the individual subunits (the last section in "RESULTS"). This result suggests that the AMP functions to accelerate the assembly rather than the subunit folding. Investigation of this point is in progress. In addition, we showed that neither FAD nor the partner subunit alters the folding reaction of the subunit. These observations can be compared with the findings by Kuwajima *et al.* for parvalbumin (*23*) and α-lactalbumin (*24*). The refolding of these Ca^{2+}-binding proteins are accelerated in the presence of Ca^{2+} ion. Kuwajima *et al.* explained this phenomenon in terms of the affinity of Ca^{2+} for the transition state between the I and N states: Ca^{2+} ion lowers the free energy of the transition state by binding to it and thus decreases the activation energy. In this context, our present results are interpreted as indicating that the transition state of each subunit of ETF interacts with none of the other components. This is reasonable, because even the N form of each subunit shows no detectable binding with either FAD or AMP (*9*), and very weak binding with the partner subunit (our unpublished data): tight binding has been observed only in the presence of both the refolded subunits and at least one ligand (namely, $\alpha+\beta+$AMP, $\alpha+\beta+$FAD, or $\alpha+\beta+$AMP+FAD) (*9*).

REFERENCES

1. Crane, F.L. and Beinert, H. (1956) On the mechanism of dehydrogenation of fatty acyl derivatives of coenzyme A: II. The electron-transferring flavoprotein. *J. Biol. Chem.* **218**, 717-731
2. Furuta, S., Miyazawa, S., and Hashimoto, T. (1981) Purification and properties of rat liver acyl-CoA dehydrogenases and electron transfer flavoprotein. *J. Biochem.* **90**, 1739-1750
3. Gorelick, R.J., Mizzer, J.P., and Thorpe, C. (1982) Purification and properties of electron-transferring flavoprotein from pig kidney. *Biochemistry* **21**, 6936-6942
4. Husain, M. and Steenkamp, D.J. (1983) Electron transfer flavoprotein from pig liver mitochondria: A simple purification and re-evaluation of some of the molecular properties. *Biochem. J.* **209**, 541-545
5. McKean, M.C., Beckmann, J.D., and Frerman, F.E. (1983) Subunit structure of electron transfer flavoprotein. *J. Biol. Chem.* **258**, 1866-1870
6. Sato, K., Nishina, Y., and Shiga, K. (1993) Electron-transferring flavoprotein has an AMP-binding site in addition to the FAD-binding site. *J. Biochem.* **114**, 215-222
7. DuPlessis, E.R., Rohlfs, R.J., Hille, R., and Thorpe, C. (1994) Electron-transferring flavoprotein from pig and the methylotrophic bacterium W3A1 contains AMP as well as FAD. *Biochem. Mol. Biol. Int.* **32**, 195-199
8. Roberts, D.L., Herrick, K.R., Frerman, F.E., and Kim, J.-J.P. (1995) Crystallization and preliminary X-ray analysis of electron transfer flavoproteins from human and *Paracoccus denitrificans*. *Protein Sci.* **4**, 1654-1657
9. Sato, K., Nishina, Y., and Shiga, K. (1994) Preparation of separated α and β subunits of electron-transferring flavoprotein in unfolded forms and their restoration to the native holoprotein form. *J. Biochem.* **116**, 147-155
10. Kuwajima, K. (1989) The molten globule state as a clue for understanding the folding and cooperativity of globular-protein structure. *Proteins: Structure, Function, and Genetics* **6**, 87-103
11. Ptitsyn, O.B., Pain, R.H., Semisotnov, G.V., Zerovnik, E., and Razgulyaev, O.I. (1990) Evidence for a molten globule state as a general intermediate in protein folding. *FEBS Lett.* **262**, 20-24
12. Ohgushi, M. and Wada, A. (1983) 'Molten-globule state': A compact form of globular proteins with mobile side-chains. *FEBS Lett.* **164**, 21-24
13. Sato, K., Nishina, Y., Shiga, K., Tojo, H., and Tada, M. (1991) The existence of two different forms of apo-electron-transferring flavoprotein. *J. Biochem.* **109**, 734-740
14. Walsh, C., Fisher, J., Spencer, R., Graham, D.W., Ashton, W.T., Brown, J.E., Brown, R.D., and Rogers, E.F. (1978) Chemical and enzymatic properties of riboflavin analogues. *Biochemistry* **17**, 1942-1951
15. Bock, R.M., Ling, N.-S., Morell, S.A., and Lipton, S.H. (1956) Ultraviolet absorption spectra of adenosine-5′-triphosphate and related 5′-ribonucleotides. *Arch. Biochem. Biophys.* **62**, 253-264
16. Greenfield, N., Davidson, B., and Fasman, G.D. (1967) The use of computed optical rotatory dispersion curves for the evaluation of protein conformation. *Biochemistry* **6**, 1630-1637
17. Pace, C.N. (1986) Determination and analysis of urea and guanidine hydrochloride denaturation curves. *Methods Enzymol.* **131**, 266-280
18. Matthews, C.R. (1987) Effect of point mutations of the folding of globular proteins. *Methods Enzymol.* **154**, 498-511
19. Cowgill, R.W. (1968) Fluorescence and protein structure. XV. Tryptophan fluorescence in a helical muscle protein. *Biochim. Biophys. Acta* **168**, 431-438

20. Cowgill, R.W. (1967) Fluorescence and protein structure. X. Reappraisal of solvent and structural effects. *Biochim. Biophys. Acta* **133**, 6-18
21. Schellman, J.A. (1987) The thermodynamic stability of proteins. *Annu. Rev. Biophys. Biophys. Chem.* **16**, 115-137
22. Schellman, J.A. (1987) Selective binding and solvent denaturation. *Biopolymers* **26**, 549-559
23. Kuwajima, K., Sakuraoka, A., Fueki, S., Yoneyama, M., and Sugai, S. (1988) Folding of carp parvalbumin studied by equilibrium and kinetic circular dichroism spectra. *Biochemistry* **27**, 7419-7428
24. Kuwajima, K., Mitani, M., and Sugai, S. (1989) Characterization of the critical state in protein folding. Effect of guanidine hydrochloride and specific Ca^{2+} binding on the folding kinetics of α-lactalbumin. *J. Mol. Biol.* **206**, 547-561